Journal of
Materials Chemistry B

PAPER

View Article Online
View Journal | View Issue

Cite this: J. Mater. Chem. B, 2016, 4, 431

Different chemical strategies to aminate oxidised multi-walled carbon nanotubes for siRNA complexation and delivery†

Cinzia Spinato,[a] Davide Giust,[b] Isabella Anna Vacchi,[a] Cécilia Ménard-Moyon,[a] Kostas Kostarelos[b] and Alberto Bianco*[a]

Received 7th October 2015,
Accepted 3rd December 2015

DOI: 10.1039/c5tb02088c

www.rsc.org/MaterialsB

In this work, we have investigated the preparation of amino-functionalised multi-walled carbon nanotubes (MWCNTs) as potential carriers for the delivery of siRNA. Several studies have shown promising results exploiting functionalised CNTs for the delivery of genetic material *in vitro* and *in vivo*. Our groups have previously observed that the type of surface functionalisation used to modify oxidised MWCNTs (oxMWCNTs) can lead to significant differences in nanotube cellular uptake and delivery capability. In those studies, amino-functionalised CNTs were obtained by cycloaddition reactions. Here, we focused on the direct conversion of the carboxylic groups present on oxMWCNTs into amines, and we attempted different synthetic strategies in order to directly tether the amines onto the CNTs, without extending the lateral chain. The functionalised material was characterised by X-ray photoelectron spectroscopy, Fourier transform infra-red spectroscopy and transmission electron microscopy, and the most water-dispersible CNTs were selected for siRNA complexation and cellular uptake studies. The aminated conjugates are demonstrated to be promising vectors to achieve intracellular transport of genetic information.

Introduction

A lot of research has been devoted to investigate the possibility of employing carbon nanotubes (CNTs) as nanovectors for drug or gene delivery.[1–5] When properly functionalised, their unique physicochemical and structural properties are matched with good biocompatibility,[6,7] cell membrane penetration ability[8,9] and rapid excretion,[10] making nanotubes very appealing as delivery systems. It is now established that the external chemical modification of carbon nanotubes is necessary for their employment in bioapplications. Indeed, it allows increased water dispersibility by partially or totally disentangling the CNT bundles,[11] and it substantially reduces CNT toxicity.[12–15] Moreover, functionalised CNTs have shown excellent immunomodulatory properties, that could be exploited in immunotherapy and delivery of vaccines.[7,16,17] Most approaches for covalent functionalisation of CNTs start from their preliminary oxidation through acid treatment. This strategy introduces a large number of carboxylic groups at the CNT tips, and concurrently increases their solubility, shortens and introduces defects on the aromatic honeycomb structure. Length and degree of defects play a major role in the use of CNTs as delivery systems, in fact it has been already reported that short CNTs bearing defects are more easily uptaken by cells.[18–20]

In our previous studies we demonstrated that covalently functionalised CNTs are able to translocate the plasma membrane and achieve intracellular delivery of genetic material, such as plasmid DNA or small interfering RNA (siRNA).[8,21–23] We have shown that CNTs functionalised with terminal amino groups can form stable complexes with siRNA. Amino-functionalised multi-walled carbon nanotubes (MWCNTs) (named MWCNT-NH_3^+) were used to deliver a toxic siRNA sequence to a human lung tumour xenograph model by intratumoural injection, leading to tumour growth inhibition and prolonged animal survival.[21] In another study from our groups, the same type of amino-functionalised MWCNTs were able to afford therapeutic gene silencing in neuronal tissue by delivery of siRNA in an induced stroke model, resulting in functional rehabilitation of diseased rodents.[22] In a very recent work, we proved that the complexation of a siRNA sequence onto MWCNT-NH_3^+ facilitated its internalisation by tumour cells in solid tumour mass *in vivo*, resulting in a significant knockdown of the corresponding gene.[23] The ability of these CNT-based cationic

[a] CNRS, Institut de Biologie Moléculaire et Cellulaire, Laboratoire d'Immunopathologie et Chimie Thérapeutique, 67000 Strasbourg, France. E-mail: a.bianco@ibmc-cnrs.unistra.fr
[b] Nanomedicine Laboratory, Faculty of Medical & Human Sciences and National Graphene Institute, University of Manchester, AV Hill Building, Manchester M13 9PT, UK

† Electronic supplementary information (ESI) available. See DOI: 10.1039/c5tb02088c

conjugates to silence cytotoxic genes makes them promising carriers for genetic material. Indeed, the poor stability of siRNA in the cytoplasmic media hampers its efficient delivery *in vivo*, and continues to prompt researches toward the design of delivery systems able to translocate high doses of siRNA directly into the cytoplasm.[24–26] To this purpose, the presence of positively charged amino groups on the surface of CNTs is essential for an efficient complexation with nucleic acids.

Based on previous findings, we wanted to investigate more in detail the nanotube structure–cell delivery relationship by preparing a novel type of amino-MWCNT carrier. Specifically, our aim was to achieve the direct conversion of the carboxylic groups of oxidised MWCNTs (oxMWCNTs) into amino groups without extension of the alkyl chain. In all our previous reports, aminated CNTs were prepared either by cycloaddition reaction or by amidation of the carboxylic functions (or a combination of the two). These approaches contemplate the attachment of an amine-terminating linker, thus extending the distance between the amino groups and the CNT surface.[8,12,13,21,22,27,28] Moreover, in one of our recent studies, we observed that oxidised MWCNTs can trigger a sustained inflammatory response in brain tissues, whereas ammonium-functionalised MWCNTs were better tolerated.[28] Therefore, increasing the amount of positively charged groups (*i.e.* ammonium over carboxylic groups) on the nanotubes could remarkably modify and improve the toxicity profile of the carrier. We considered it interesting to explore further the relationship between surface chemistry, delivery and cellular uptake, and carry out a different investigation for the preparation of possible siRNA delivery using CNT-based carriers.

To date, reports concerning amino-modified carbon nanotubes are few due to the relative difficulty of the modification. In contrast to the rather 'rich' sidewall chemistry of CNTs, the chemistry at the tips of nanotubes has been limited only to a few reactions, mainly based on derivatisation of the carboxylic groups after oxidative purification.[29–31] Only few reports have so far investigated the possibility of directly tethering CNT ends with heteroatoms different from oxygen.[32–35] Previous attempts to directly convert carboxylic terminal groups into amines have been reported for single-walled carbon nanotubes (SWCNTs) by the Campbell group.[33] They applied for the first time in CNT chemistry the Hofmann rearrangement of primary amides and the Curtius rearrangement of acyl azides, achieving in both ways the preparation of SWCNTs with amino groups directly attached to the tube structure. Another work has described the transformation of carboxylic groups on SWCNTs into amino-methyl groups through a different multistep synthetic path, involving a phthalimide intermediate.[32] The final step of this path, however, suffers from an inappropriate protocol to remove the protection group, which requires hydrazine instead of trifluoroacetic acid. All mentioned chemical reactions were performed only on SWCNTs, while similar experiments have so far not been carried out on MWCNTs yet, nor envisaged any bio-application. Therefore further investigations on this area are undoubtedly needed and could help to achieve a better understanding of the surface chemistry of oxMWCNTs.

This work aimed at exploring the chemical conversion of carboxylic groups of MWCNTs into amines through different synthetic strategies. Amino-functionalised MWCNTs were characterised by X-ray photoelectron spectroscopy (XPS), transmission electron microscopy (TEM) and Fourier transform infra-red spectroscopy (FT-IR). We have then assessed the behaviour of these amino-functionalised MWCNTs toward siRNA complexation and evaluated the uptake of these complexes by lung cancer cells.

Experimental part

Materials and methods

The chemicals and solvents were obtained from commercial suppliers and used without further purification. MWCNTs were purchased from *Nanostructured & Amorphous Materials Inc.* (20–30 nm diameter, 0.5–2 μm length, 95% purity; stock # 1240 XH), and they were produced by catalytic carbon vapour deposition (CCVD). The solvents used for synthesis were analytical grade. When anhydrous conditions were required, high quality commercial dry solvents were used. Water was purified using a Millipore filter system milli-Q®. When stated, suspensions were sonicated in a water bath (20 W, 40 kHz). For CNT filtration, PTFE membrane from Millipore were employed. Membranes for dialysis (MWCO 12 000–14 000 Da) were purchased from Spectrum Laboratories, Inc. FT-IR spectra were measured on a Perkin Elmer Spectrum One ATR-FT-IR spectrometer. XPS analyses were performed on a Thermo Scientific K-Alpha X-ray photoelectron spectrometer equipped with an Al anode as the X-ray source (X-ray radiation of 1486 eV) and with a basic chamber pressure of $\sim 10^{-8}$–$10.^{-9}$ mbar. Spot sizes of 400 μm were used. Survey spectra are an average of 10 scans with a pass energy of 200.00 eV and a step size of 1 eV. High-resolution spectra are an average of 10 scans with a pass energy of 50.00 eV and a step size of 0.1 eV. Reported spectra and values are obtained from the average of measurements performed on two different spots of the sample. TEM analysis was performed on a Hitachi H7500 microscope (Tokyo, Japan) with an accelerating voltage of 80 kV, equipped with an AMT Hamamatsu camera (Tokyo, Japan). The samples were dispersed in water/MeOH (1 : 1) at a concentration of 0.05 mg mL^{-1} and the suspensions were sonicated for 15 min. Ten microliters of the suspensions were drop-casted onto carbon-coated copper grids (Formvar/Carbon 300 Mesh, Cu from Delta Microscopies) and left for evaporation under ambient conditions. For the electrophoresis and uptake experiments, the nanotubes were dispersed in ultrapure water and the dispersions were treated in sterile conditions for cell culture.

Oxidation of MWCNTs. 500 mg of pristine MWCNTs were treated with a solution of H_2SO_4/HNO_3 (75 mL, 3 : 1 v/v, 98% and 65%, respectively), and the mixture was sonicated for 24 h in a water bath (20 W, 40 kHz). The mixture was then carefully diluted with distilled water (300 mL) and filtered through a PTFE membrane (0.45 μm). The black material on the filter membrane was re-suspended in water by sonicating for 15 min

and filtered again, and this sequence was repeated until neutrality of the aqueous solution. The CNTs were then further purified by dialysis against deionised water for 48 h and finally lyophilised. Shortened oxidised MWCNTs (oxMWCNTs **1**) were obtained with a yield of 98% w/w. The average length distribution of oxMWCNTs was assessed to be 381 nm by TEM. The amount of carboxylic acids introduced corresponds to 1.4 mmol g^{-1} and was calculated on the basis of the weight loss obtained by thermogravimetric analysis (TGA).

Activation of oxMWCNTs. oxMWCNTs **1** (160 mg) were dispersed in oxalyl chloride (80 mL) by short sonication, and the mixture was then refluxed for 24 h under argon. The solvent was removed under reduced pressure and the resulting activated nanotubes (MWCNT-COCl) were used straightaway for the following step.

Hofmann reaction

Synthesis of MWCNT-$CONH_2$. Activated oxMWCNTs (160 mg) were dispersed in dry DMF (26 mL) by sonicating for 5 min. A solution of BuOH/pyridine (Py) 1 : 2 (3 mL) was then slowly added to the dispersion at r.t. and the reaction mixture was stirred at 80 °C for 70 h under argon. The mixture was filtered through a PTFE membrane (0.45 μm), and the CNTs were re-dispersed in EtOH by sonicating for 10 min and filtered again. This washing sequence was repeated twice, and the resulting MWCNT-COOBu were directly submitted to the following step. MWCNT-COOBu were dispersed in 25% aq. NH_3 (250 mL) by sonicating for 10 min, and the reaction mixture was stirred at 40 °C for 100 h. CNTs were then recovered by filtration and washed by dispersing them in water, sonicating for 10 min and filtrating. This sequence was repeated with H_2O, EtOH (×2) and the CNTs were dried, affording 131 mg of MWCNT-$CONH_2$ **2** (yield of 82% w/w).

Hofmann rearrangement. Br_2 (2.7 mL, 53 mmol) was slowly added to a solution of CH_3ONa (4.06 g, 75 mmol) in dry MeOH (150 mL) at 0 °C under vigorous stirring in argon atmosphere. After 5 min, MWCNT-$CONH_2$ **2** (125 mg) were added to the solution, which was gently sonicated for few minutes and then refluxed overnight (70 °C) under argon. An additional aliquot of Br_2 (1.2 mL) was then added, and the mixture was stirred at 70 °C for additional 20 h. The product was recovered by filtration, washed with saturated $NaHCO_3$ (×3), H_2O, EtOH and acetone, and finally dried *in vacuo*, affording aminated MWCNTs **3** (yield of 98% w/w).

Curtius rearrangement

Sodium azide (26 mg) was added to a dispersion of MWCNT-COCl (10 mg) in dry DMF (10 mL), and the mixture was stirred at r.t. for 45 h, and then at 100 °C for 20 h, under argon. The mixture was then filtered through a PTFE membrane (0.45 μm), and the CNTs were washed with DMF by sonication for 10 min and filtration, and successively treated with conc. HCl for 60 h. Aminated CNTs were recovered by filtration, and washed by dispersing them in water, sonicating for 10 min and filtrating. This washing sequence was then repeated with MeOH (×2) and acetone, and MWCNTs **4** were finally dried *in vacuo*.

Hunsdiecker reaction, azidation and reduction

oxMWCNTs **1** (17 mg) were dispersed in MeCN/H_2O 97 : 3 (8 mL) by sonicating for 15 min. LiOAc (6 mg) and *N*-iodosuccinimide (150 mg) were then added to the mixture and this was stirred at 60 °C for 24 h. The CNTs were recovered by filtration and washed with MeCN, MeOH, and acetone (×2), and finally dried *in vacuo* obtaining iodinated MWCNTs **5**.

MWCNTs **5** (13 mg) were sonicated in dry DMF (6 mL) for 10 min under argon. NaN_3 (40 mg) was then added to the dispersion and this was stirred at r.t for 5 h and at 50 °C for 16 h. The CNTs were then recovered by filtration (0.1 μm) and washed with DMF (×2), MeOH (×2) and acetone (×2), and finally dried *in vacuo*. In a flamed round-bottom flask, MWCNT-N_3 were dispersed in freshly dried THF (10 mL) by sonicating for 20 min. A 2.2 M solution of $LiAlH_4$ in dry THF (0.8 mL) was slowly added by syringe to the CNT dispersion, which was vigorously stirred overnight. The mixture was then carefully poured into a beaker with cold water (60 mL) under stirring. Few drops of concentrated HCl were then added to the mixture to dissolve the lithium salts, and the CNTs were recovered by filtration (0.1 μm), re-dispersed in H_2O and precipitated by centrifugation. The supernatant was removed away and CNTs were further washed once with EtOH and once with acetone recovering them by precipitation. MWCNTs **6** were finally dried *in vacuo*.

Reduction and phthalimide coupling

Synthesis of MWCNT-CH_2OH. oxMWCNTs **1** (19 mg) were dispersed in dry THF (10 mL) by sonicating for 30 min under argon. A 1 M solution of $LiAlH_4$ in THF (0.4 mL) was carefully added by syringe to the dispersion and this was stirred for 1 h. The mixture was sonicated for 10 min and then slowly poured onto a 2 M HCl solution (30 mL) under vigorous stirring. The CNTs were then recovered by filtration (0.1 μm), washed with H_2O, EtOH, and acetone and dried *in vacuo*, obtaining MWCNT-CH_2OH **7**.

Phthalimide coupling. MWCNTs **7** (12 mg) were dispersed in THF (10 mL) by sonicating for 30 min under argon. Phthalimide (14 mg) and diethyl azodicarboxylate (DEAD) (2 mL) were then added, and the mixture was sonicated for 2 h and further stirred for 2.5 h. The mixture was then diluted with MeOH (50 mL), filtered (0.1 μm) and the recovered CNTs were re-dispersed in MeOH (20 mL) by sonication, filtered again and dried *in vacuo*. The so-obtained Pht-functionalised CNTs were dispersed in EtOH (10 mL) by sonication. Hydrazine hydrate (1 mL) was added to the mixture and this was stirred at r.t. overnight. Aminated CNTs **8** were recovered by filtration, washed once with EtOH, twice with MeOH and once with acetone and finally dried.

Evaluation of siRNA:MWCNT complexation by agarose gel electrophoresis mobility assay

Dilutions of non-coding siRNA (siRNAneg, Qiagen, MW = 14 857 g mol^{-1}) in RNAse-free water (20 μM) were prepared according to manufacturer protocols. Dilutions were prepared in milli-Q water in order to have a final concentration of 0.25 μg of siRNAneg in 15 μL of solution. Dilutions of aminated

MWCNTs were prepared according to each mass ratio required for the complexation with siRNAneg from a 1 mg mL^{-1} dispersion in milli-Q RNAse-free water after sonication for few minutes. Final volumes of MWCNT dilutions were set to be at 15 μL. These volumes of carbon nanotubes and siRNA were mixed together by rapidly pipetting and let interact for 30 min at r.t. prior to load into 1% agarose gel (final volume 30 μL). Before the loading of samples on the 1% agarose gel, each sample was added with 8 μL of Green Orange DNA loading dye (Fermentas, Thermo Scientific) (total loading sample volume = 38 μL). Gels were run for 45 min at 70 mV before visualisation using the GeneSnap software under UV light.[36] Gel was prepared by using TBE buffer (Tris-borate-ethylenediaminetetraacetic acid (EDTA)) added of 1% agarose. Briefly, Trizma base (108 g), boric acid (55 g), EDTA (9.3 g) and NaOH (1 g) were dissolved in 1 L of distilled water by vigorously stirring. The buffer was diluted 20× with distilled water, and the same buffer used for the 1% agarose gel preparation (30 min) as well as running buffer.

Monitoring cellular uptake of fluorescently labeled-siRNA in A459 cells by confocal microscopy

A459 lung cancer cells were maintained in complete F12-Ham's (Gibco, LifeTechnologies) media complemented with 10% FBS (foetal bovine serum) on non-coated Petri's dishes, and media renewed every 3 days until cells were at confluence. The day before the experiment, the cells were seeded at 5×10^3 cells per well density on a MILLIPORE-microscope slide multi well support (Ezslides, MILLIPORE) in the presence of complete media. Non-coding AlexaFluor546-labeled siRNAneg (siRNA-AF546) (5′-3′: UGCGCUACGAUCGACGAUG) (Eurogentec, UK) was used to complex with aminated MWCNTs, mixing equal volumes to obtain a mass ratio of 16 : 1, 48 : 1 and 96 : 1. To obtain siRNA-AF546 at final concentration of 40 nM corresponding to 0.25 μg of siRNA on each well, 75 μL of siRNA-AF546 (20 μM) was diluted in 1175 μL of RNAse free sterile water. One hundred μL of this solution were mixed with 100 μL of aminated MWCNTs diluted in sterile/RNAse free milli-Q water. These dilutions were thus mixed together by rapidly pipetting and let interact for 30 min prior being added to each well containing cells and 400 μL of FBS free complete media. Treatments at 4 h were stopped by removing the media, washing several times with sterile water, fixing cells in 4% paraformaldehyde for 15 min, removing by washing and adding 5 μL of DAPI staining for the cell nuclei. The same procedure was repeated for the 24 h treatments, but after 4 h incubation in the presence of the complexes, the medium was complemented with 10% of FBS to preserve the cell growth. Cells were then visualised under confocal microscopy by mounting the coverslip to each microscopy slide. Images were acquired on a confocal laser scanning LSM 710 microscope (Carl Zeiss) or on a Mp_OPO SP8 (Leica) used in the confocal mode.

Results and discussion

Commercially available MWCNTs were firstly oxidised by acid treatment with a HNO_3/H_2SO_4 mixture under sonication, following a common reported procedure.[37] This oxidation method allows for the further purification of pristine nanotubes, and yields shortened oxMWCNTs highly functionalised with oxygen-containing groups like carboxylic acids, located mainly at the tips.[38,39] The average length distribution of so-obtained oxMWCNTs (**1**) is 381 nm and the amount of oxygen-containing groups estimated by TGA is 1.4 mmol g^{-1}. The atomic percentage of carbon assessed by elemental analysis varies from 97.1% for pristine CNTs to 83.6% for the oxidised sample, while that of hydrogen increases from 0 to 0.7%, accounting for the hydrogen atom of the COOH group. These values are in good agreement with the elemental composition obtained by XPS analysis of oxMWCNTs **1**: 84.6% for carbon and 15.4% for oxygen (see Table 1).

Table 1 Atomic percentage of carbon, oxygen and nitrogen in oxMWCNTs and aminated MWCNTs calculated from XPS data

	Atom%		
Compound	C	O	N
oxMWCNTs **1**	84.6	15.4	—
MWCNT-NH_2 **3**	76.5	22.0	1.6
MWCNT-NH_3^+ **4**	84.8	13.9	1.3
MWCNT-NH_2 **6**	76.1	21.7	2.1
MWCNT-CH_2NH_2 **8**	81.4	15.4	3.2

For the direct conversion of the carboxylic groups of oxMWCNTs into amines we selected four different synthetic strategies: (i) Hofmann rearrangement, (ii) Curtius rearrangement, (iii) Hunsdiecker reaction, and (iv) reduction of COOH and phthalimide coupling (Schemes 1 and 2). The first two approaches, Hofmann and Curtius rearrangements, are based on the carboxylic group activation through acylation and occur *via* an isocyanate intermediate.[40] The third strategy features halodecarboxylation (Hunsdiecker reaction), successive substitution of the halide by an azide and reduction into an amine. In the last approach, the reduction of the carboxyl is followed by amination through phthalimide introduction. We proceeded with the complete characterisation only for the final compounds and the relevant stable intermediates.

Chemical modification

Approaches (i) and (ii) both start from the conversion of the carboxylic acid into acyl chloride by treatment of compound **1** with neat oxalyl chloride. After solvent removal, MWCNT-COCl were immediately subjected to the subsequent steps (path i or ii of Scheme 1) following the procedures reported by Gromov and coworkers.[33]

For the approach involving Hofmann rearrangement (path i), the activated carboxylic group was transformed into amide (compound **2**) by conversion into a butyl ester and successive treatment with aqueous ammonia. Under dry conditions, the amide can undergo Hofmann rearrangement into isocyanate, which is quickly hydrolysed into primary amine (compound **3**). The second strategy (ii) instead, involves the derivatisation of the acyl chloride into acyl azide, which by Curtius rearrangement affords an isocyanate intermediate. This undergoes acid hydrolysis into primary amine (compound **4**).

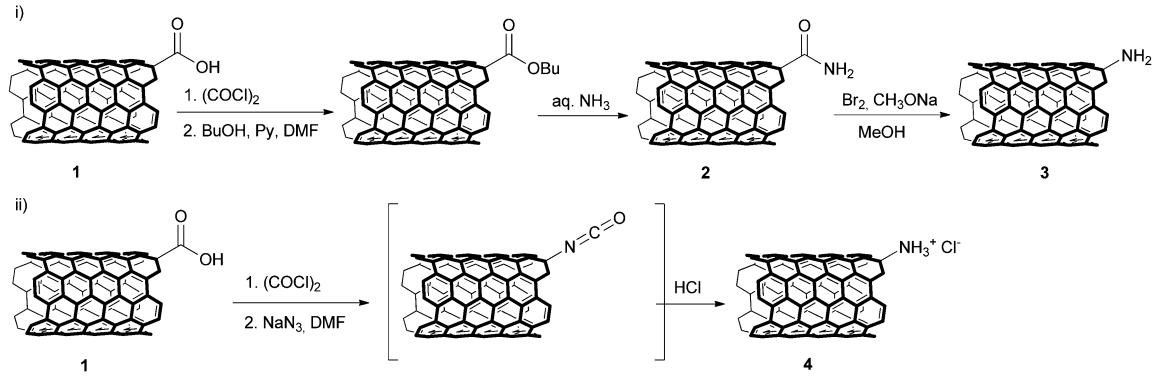

Scheme 1 Acylation of carboxylic group and conversion into amino group: (i) *via* Hofmann rearrangement of the amide, (ii) *via* Curtius rearrangement of the isocyanate intermediate. For clarity, only one functional group is represented on the nanotube.

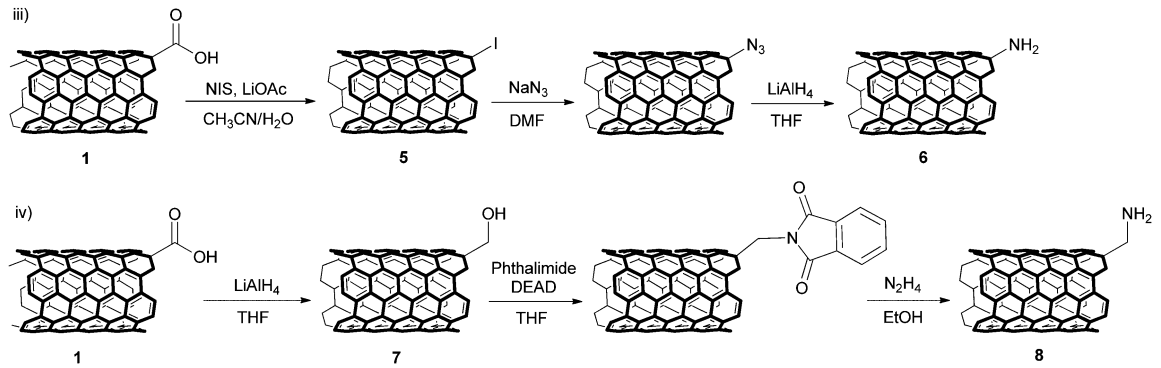

Scheme 2 Conversion of carboxylic acid (iii): *via* Hunsdiecker reaction and (iv) *via* oxMWCNT reduction and phthalimide coupling.

Hunsdiecker reaction is a well-known method to form an alkyl or an aryl halide starting from a carboxylic acid, decreasing the length of the alkyl chain by one carbon unit.[40] Several variations and modifications of the original Hunsdiecker reaction have been so far investigated to avoid the employment of very sensitive silver salts.[41–43] One example of a modified Hunsdiecker reaction has been reported for the iodination of oxidised SWCNTs by Coleman and coworkers.[35] We decided to apply to MWCNTs a variation of the Hunsdiecker reaction, which was reported by Roy's group to work efficiently with unsaturated carboxylic acid.[42] oxMWCNTs **1** were reacted with *N*-iodosuccinimide (NIS) and catalytic LiOAc to afford iodinated MWCNTs **5** (Scheme 2, path iii). The nucleophilic substitution of iodine into azide was followed by azide reduction with lithium aluminium hydride to obtain amino-functionalised MWCNTs **6**.

In the last approach we slightly modified the synthetic strategy reported by Brinson and coworkers for the preparation of amino-functionalised SWCNTs.[32] This consists in the reduction of the carboxylic group to hydroxyl, followed by phthalimide coupling and hydrolysis to finally afford an amino methyl group (Scheme 2, path iv). The so-obtained compound **8** is the only one among the synthesised amino-functionalised MWCNTs, which upon conversion is featuring the amine group detached from the aromatic nanotube structure by one carbon unity, the methylene group.

Characterisation

Rigorous characterisation of the surface composition of modified carbon nanotubes is critical to their further employment, both for material and bioapplications. Chemical derivatisation of CNTs at their tips occurs through the conversion of the carboxylic groups, however the conversion is usually not total, meaning that not all carboxylic groups undergo reaction.[37] For the characterisation of the four aminated MWCNTs, we had to exclude TGA because of minor weight difference with the starting material. Furthermore, the direct bond between the amino group and the nanotube structure likely results in a high percentage of aromatic amines, which cannot be quantified by the common colorimetric Kaiser test.[44] This test, in fact, only allows to quantify primary aliphatic amines. Even in the case of compound **8**, where the amino groups are primary aliphatic amines, Kaiser test resulted negative. We can speculate that either the proximity of the aromatic structure affects the amine reactivity, or the location of the amino groups next to the nanotubes hampers the reaction with ninhydrin. Nevertheless, XPS and FT-IR spectroscopy are very sensitive techniques and represent powerful tools for surface characterisation of carbon nanotubes, allowing the detection of nitrogen atoms and amine-containing groups, respectively.

Surface characterisation (XPS and FT-IR spectroscopy)

X-ray photoelectron analysis allows to investigate the surface chemical composition of carbon nanomaterials and obtain

information about the nature of functional groups (see ESI,† Fig. S1). In Table 1 are reported the atomic percentage of C, O and N for the different samples. After the chemical modification to introduce the amine groups, nitrogen was detected in all samples, and a concomitant decrease in the atomic percentage of either carbon or oxygen was observed. In the four samples of

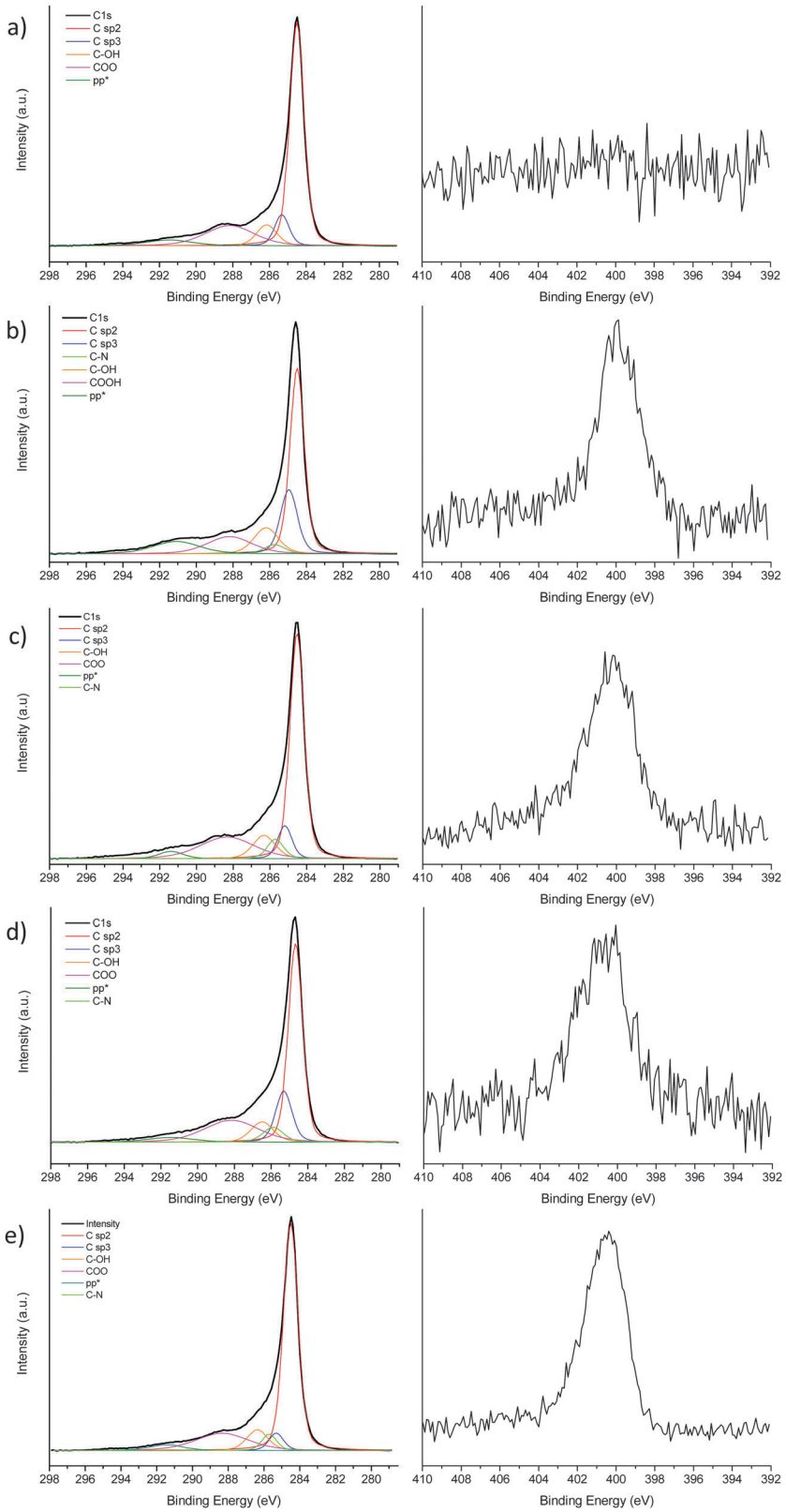

Fig. 1 XPS spectra of C1s (left side) and N1s (right side) of oxMWCNTs (a) and aminated compounds **3** (b), **4** (c), **6** (d) and **8** (e).

aminated MWCNTs the percentage of nitrogen ranges between 1.3 and 3.2%, indicating that only a small amount of carboxylic groups were efficiently converted into amino groups.

By deconvolution of the C1s curve of oxidised MWCNTs **1** we could identify the contributions given by the different functional groups (Fig. 1a). Aside from the main peak at 284.5 eV due to sp^2 C–C bonds, additional features at 285.3, 286.1 and 288.2 eV are present, which were assigned to sp^3 C, –*C*–O (alcohol) and O–*C*=O (carboxyl and ester), respectively.[45] Finally, at 291.5 eV appears the π–π* satellite band, which is typical of the aromatic structures of carbon nanotubes.[46] When deconvoluting the C1s curves of the aminated compounds, a good fitting was possible only including the component of the *C*–N bond, with energy between 284.9–285.9 eV, the intensity of which varies around 4–7% (Fig. 1b–e). The N1s spectra of the four MWCNT-NH_2 samples display the respective nitrogen peak centred at 400 eV (Fig. 1), which is in agreement with the expected value for primary amines.[32,47]

Infrared spectroscopy

In the FT-IR spectrum of oxMWCNTs **1** (Fig. 2) we can clearly recognize the typical features of oxidised nanotubes: the broad band at 3430 cm^{-1} and the peak at 1584 cm^{-1} determined by the stretching vibration of OH of the carboxylic groups and the C=C bendings.[48,49] Moreover, the small shoulder around 1700 cm^{-1} can be attributed to the C=O stretching of the carboxylic groups. In aminated MWCNTs **3** the presence of amine groups is confirmed by the appearance of an intense band at 1365 cm^{-1}, due to the C–N stretching, and smaller peaks at 841 and 701 cm^{-1}, from the NH_2 bending out-of-plane. The shoulder band at 1668 cm^{-1} can also be attributed to the scissoring of primary amines. Similarly, the FT-IR spectra of MWCNT-NH_2 **4** exhibits new bands at 1198 and 1085 cm^{-1} from the C–N stretching vibrations. The IR absorption of MWCNT-NH_2 **6** also displays changes in the range between 1250 and 950 cm^{-1}, which are attributed to the C–N stretching. In the spectra of almost all conjugates we can remark the persistence of a small band around 1700 cm^{-1}, which could be assigned to the residual carboxylic groups.

Finally, compound **8**, which is the only one displaying methyleneamino groups, shows several bands originated from the C–N stretching vibrations (1588, 1423 and 1049 cm^{-1}). Moreover, around 2919 cm^{-1} appears a new absorption feature, which accounts for the stretching of C–H, thus confirming the presence of the methylene moiety. In general, the FT-IR spectra of amine-functionalised MWCNTs obtained by the four different strategies all show new absorption bands compared to the starting oxMWCNTs, and their spectral features are relatively similar between each other, giving a further proof of the partial conversion of carboxylic groups into amines.

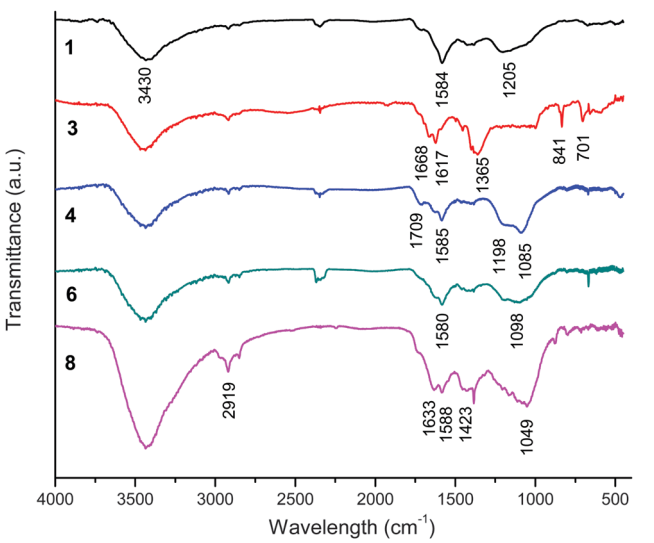

Fig. 2 FT-IR spectra of oxMWCNTs **1** (top) and aminated MWCNTs **3**, **4**, **6** and **8**.

Morphological characterisation

The average length distribution after the oxidative process was assessed by TEM and corresponds to 381 nm. From Fig. 3 it is also visible that oxMWCNTs are quite individualised and that their morphology after derivatisation is unchanged.

For the employment of CNTs in bioapplication and for their further use as carriers, it is imperative that the CNT conjugates are very well-dispersed in aqueous solutions. The water dispersibility of the amino-functionalised MWCNTs was tested by preparing 0.2 mg mL^{-1} dispersion of each compound in distilled deionised water (ddH_2O), and compared to that of oxMWCNTs **1**. From Fig. 4 it is clear that all amine-functionalised compounds maintained a very good water-dispersibility after derivatisation and are therefore suitable for our purposes.

Biological investigations

RNA interference has become one of the most powerful tools to silence specific genes.[50–52] The advantage offered by siRNA constructs lies in the fact that they act in the cell cytoplasm[50] compared to plasmid DNA that has to be delivered in the nucleus to exert its transcriptional activity. In this direction, we studied the ability of these newly synthesised aminated MWCNT constructs to bind siRNA and transport this biomolecule inside cancer cells.

Electrophoretic agarose gel mobility assay of siRNA:CNT complexes

The agarose gel electrophoretic mobility assay has been extensively used for the characterisation of nucleic acid complexation. It was applied here to monitor the degree of electrostatic complexation of siRNA onto the different aminated MWCNTs (Fig. 5).[36] Briefly, a fixed concentration (0.25 μg) of non-coding siRNA (siRNAneg) was mixed with increasing concentrations of aminated MWCNTs, and then allowed to electrostatically interact for 30 min at room temperature. The siRNA:CNT complexes were then allowed to migrate through a pre-formed 1% agarose gel upon application of an electric potential. The bright spots at the bottom of the gel indicate the free (uncomplexed) siRNA that was free to migrate. For compounds **3** and **6**, we can notice that the intensity of the siRNA bands sensibly decreases for higher concentrations of CNTs. The less intense the band appears, the more siRNA was complexed

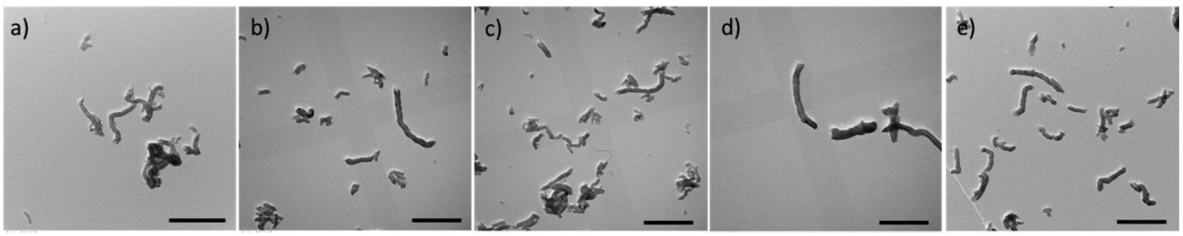

Fig. 3 TEM images of oxMWCNTs **1** (a) and aminated MWCNTs **3** (b), **4** (c), **6** (d) and **8** (e). Scale bars correspond to 500 nm.

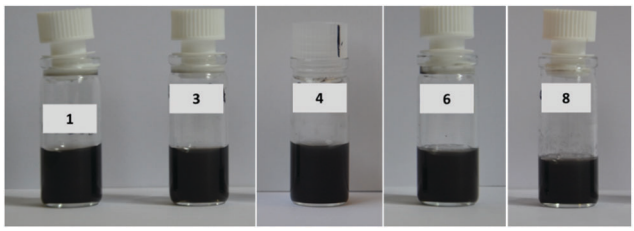

Fig. 4 Dispersions of oxMWCNTs **1** and amino-functionalised MWCNTs **3**, **4**, **6** and **8** in ddH_2O after 15 min sonication. Pictures taken 5 min after sonication.

by the CNTs, leaving only a small amount of unbound siRNA free to migrate. Therefore, MWCNTs **3** and **6** show the best complexation ability toward siRNA, with the most efficient complexation mass ratio being 1:16. In fact, at higher ratios there are no more significant changes in the band intensities. MWCNTs **4** showed a limited capacity to bind siRNA, while MWCNTs **8** failed to complex siRNA, since the band of siRNA appears as intense for the complexes as for the control (1:0 mass ratio).

Cellular uptake of siRNA:MWCNT complexes by confocal microscopy in A549 cells

Compound **3** was then selected to evaluate the ability of aminated MWCNTs to deliver the siRNA payloads into lung epithelial cells (A549). A549 cells were chosen as a well-studied human tissue culture model able to endocytose nanoparticles efficiently without being a professional phagosome, therefore excluding phagocytosis as a potential mechanism of cell internalisation. A non-coding fluorescently labeled siRNA, siRNA-AF546 (siRNA-AlexaFluor546-labeled), was allowed to complex with compound **3** at 1:16, 1:48 and 1:96 mass ratios. Cells were then incubated for 4 h and 24 h in the presence of the pre-formed siRNA-AF546:**3** complexes and the intracellular delivery of fluorescently-labelled siRNA-AF546 was evaluated by confocal microscopy. Confocal microscopy was chosen in order to obtain proof-of-principle data on the intracellular transport of siRNA and the capacity to distinguish between cytoplasmic and membrane-bound signals. In order to label cell nuclei, DAPI (4′,6-diamidino-2-phenylindole) was used for staining due to its very photostable signal useful under confocal conditions and in the presence of materials that can quench optical signals such as carbon nanotubes. Furthermore, DAPI offered a very simple protocol to be used after cell fixation without the need for cell permeabilisation. The time points chosen represented early and late points after possible internalisation. The intracellular fluorescent signal from the siRNA appeared at 4 h and reached maximum intensity at 24 h. A control experiment allowed demonstration of the poor uptake of siRNA alone (see ESI,† Fig. S2) after 4 h and 24 h incubation. In comparison to siRNA-AF546 alone, siRNA-AF546:**3** complexes were instead substantially taken up by the A549 cells after 4 h, as proved by the increased intensity of the red signal co-localised with the

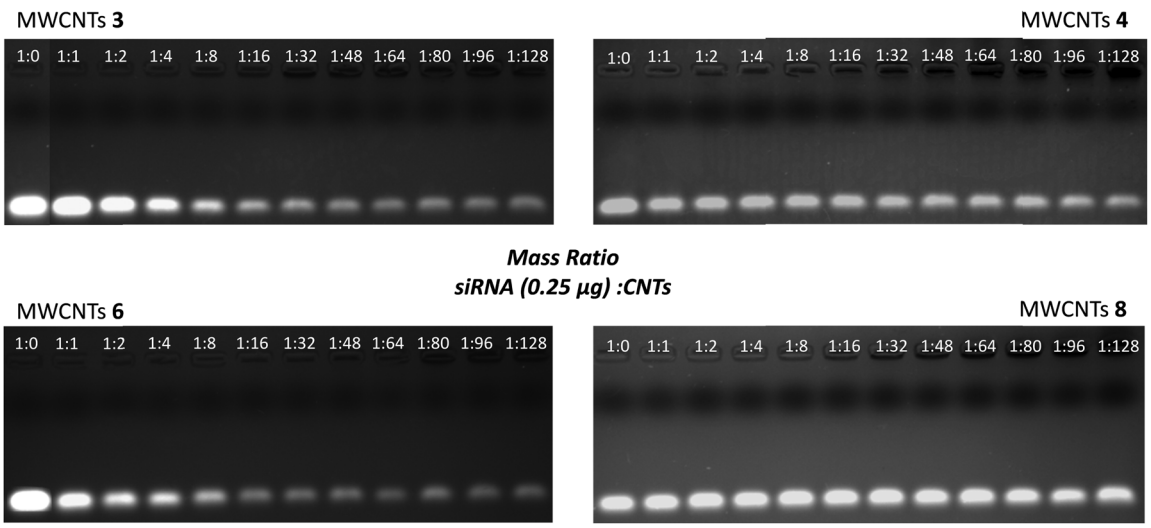

Fig. 5 Electrophoretic mobility agarose gels obtained by loading non-coding siRNA:MWCNT complexes at increasing mass ratio of nanotubes. Decreasing of the intensity of the siRNA band in the gel indicates complexation with carbon nanotubes. Mass ratio 1:0 corresponds to siRNA migrating alone (control).

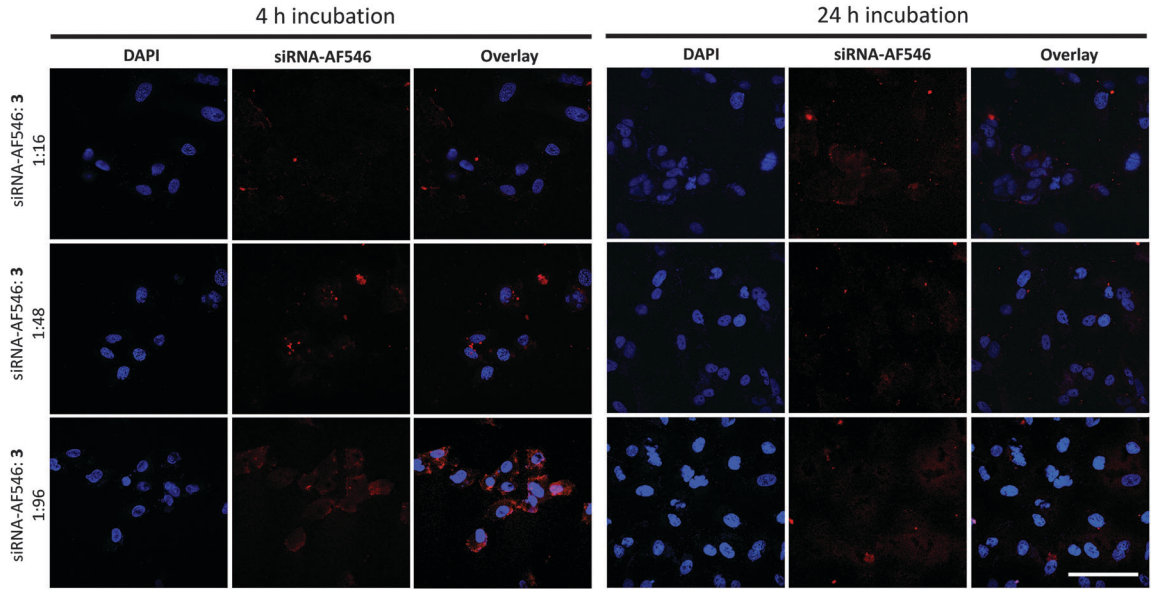

Fig. 6 Cellular uptake of siRNA-AF546:MWCNT **3** complexes in A549 cells. Pictures were obtained by confocal microscopy after exposing A549 cells for 4 h and 24 h to pre-formed siRNA-AF546:MWCNT **3** complexes at a fixed concentration of siRNA-AF546 (0.25 μg) and at increasing concentrations of MWCNT **3**, as indicated by mass ratios in the figure. Cellular uptake of the complexes can be visualised by the presence of red signal corresponding to AlexaFluor546-labeled siRNA entering the cytosol of the cells. Cell nuclei were stained by DAPI (blue). The scale bar is the same for all panels and corresponds to 50 μm.

cytosolic compartments surrounding the nuclei (Fig. 6). The accumulation of siRNA-AF546 into the cytosol increased when cells were treated with increasing ratios of aminated MWCNTs. The cellular uptake after 24 h shows that the delivery of siRNA can be sustained over time by using MWCNTs **3** as vector, without leading to significant differences in the intensity of the signal (Fig. 6).

Remarkably, low concentration of siRNA:CNT complexes afforded a relevant cellular uptake. In fact, mass ratios of 1:16, 1:48 and 1:96 correspond to 4, 12 and 24 μg of nanotubes, respectively. In addition, as evident from confocal microscopy images, the morphology of the cells was preserved after the uptake of the complexes, and this can be considered a good indication of no cytotoxic response. From these results we can conclude that the aminated MWCNT conjugate **3** was able to efficiently deliver siRNA into this specific cell line (A549) in an extent comparable to that of ammonium-functionalised nanotubes reported in our previous works.[21,27]

This study confirms the importance of selecting the most appropriate chemical approach to obtain modified MWCNTs with high aqueous dispersibility, good ability to bind siRNA and efficient intracellular delivery. In this context, it has been revealed that the distance between CNTs and terminal positively charged groups can play a crucial role to engineering vectors displaying either better siRNA complexation and delivery[27] or low cytotoxicity.[28]

Conclusion

We have designed and explored different synthetic strategies to achieve direct conversion of the carboxylic groups of oxMWCNTs into amino groups, without extending the lateral chain. The surface and morphological characterisation of all the final compounds was carried out by different techniques (XPS, FT-IR spectroscopy, TEM). On the basis of the performed characterisation it is clear that modifications have occurred for all samples and nitrogen has been introduced onto MWCNTs. However, the degree of conversion of –COOH into $–NH_2$ is not very high, meaning that a significant amount of carboxylic groups are probably still present. Although it was not possible to straightforward assess the amount and type of functionalities introduced, it is reasonable to believe that they consist of amino groups. By gel electrophoresis, we proved that two of the aminated conjugates could efficiently complex siRNA and a fluorescent complex of siRNA:CNT was able to transfect the genetic payload inside a tumour cell line without showing any sign of toxicity. We have thus showed that these novel aminated MWCNTs could represent an efficient tool to achieve the delivery of siRNA into cells.

In this study we confirmed the importance of surface chemistry and its impact on the behaviour of MWCNTs in a biological context. Clearly, the presence of positively charged groups on the surface plays a major role for the siRNA complexation/delivery, but further investigations are undoubtedly needed. In particular, we would like to stress on the importance of thorough characterisation of the CNT conjugates, which is mandatory for their possible application as vectors of genetic material.

Acknowledgements

This work was supported by the Centre National de la Recherche Scientifique (CNRS), by the Agence Nationale de la Recherche (ANR) through the LabEx project Chemistry of

Complex Systems (ANR-10-LABX-0026_CSC) and by the International Center for Frontier Research in Chemistry (icFRC). The authors wish also to acknowledge support from the European Union FP7 RADDEL program (ITN Marie Curie Actions PEOPLE-2011-290023). C. Spinato is recipient of a fellowship from the European Union (ITN Marie Curie Actions PEOPLE-2011-290023).

References

1 W. Zhang, Z. Zhang and Y. Zhang, *Nanoscale Res. Lett.*, 2011, **6**, 555.
2 E. Heister, E. W. Brunner, G. R. Dieckmann, I. Jurewicz and A. B. Dalton, *ACS Appl. Mater. Interfaces*, 2013, **5**, 1870–1891.
3 K. Bates and K. Kostarelos, *Adv. Drug Delivery Rev.*, 2013, **65**, 2023–2033.
4 G. Hong, S. Diao, A. L. Antaris and H. Dai, *Chem. Rev.*, 2015, **115**, 10816–10906.
5 L. G. Delogu, A. Magrini, A. Bergamaschi, N. Rosato, M. I. Dawson, N. Bottini and M. Bottini, *Bioconjugate Chem.*, 2009, **20**, 427–431.
6 A. Bianco, K. Kostarelos and M. Prato, *Chem. Commun.*, 2011, **47**, 10182–10188.
7 M. Orecchioni, D. Bedognetti, F. Sgarrella, F. M. Marincola, A. Bianco and L. Delogu, *J. Transl. Med.*, 2014, **12**, 138.
8 D. Pantarotto, R. Singh, D. McCarthy, M. Erhardt, J.-P. Briand, M. Prato, K. Kostarelos and A. Bianco, *Angew. Chem., Int. Ed.*, 2004, **43**, 5242–5246.
9 Q. Mu, D. L. Broughton and B. Yan, *Nano Lett.*, 2009, **9**, 4370–4375.
10 H. Ali-Boucetta and K. Kostarelos, *Adv. Drug Delivery Rev.*, 2013, **65**, 2111–2119.
11 A. Battigelli, C. Ménard-Moyon, T. Da Ros, M. Prato and A. Bianco, *Adv. Drug Delivery Rev.*, 2013, **65**, 1899–1920.
12 K. Kostarelos, L. Lacerda, G. Pastorin, W. Wu, S. Wieckowski, J. Luangsivilay, S. Godefroy, D. Pantarotto, J.-P. Briand, S. Muller, M. Prato and A. Bianco, *Nat. Nanotechnol.*, 2007, **2**, 108–113.
13 K. T. Al-Jamal, A. Nunes, L. Methven, H. Ali-Boucetta, S. Li, F. M. Toma, M. A. Herrero, W. T. Al-Jamal, H. M. M. ten Eikelder, J. Foster, S. Mather, M. Prato, A. Bianco and K. Kostarelos, *Angew. Chem., Int. Ed.*, 2012, **51**, 6389–6393.
14 H. Ali-Boucetta, A. Nunes, R. Sainz, M. A. Herrero, B. Tian, M. Prato, A. Bianco and K. Kostarelos, *Angew. Chem., Int. Ed.*, 2013, **52**, 2274–2278.
15 L. G. Delogu, E. Venturelli, R. Manetti, G. A. Pinna, C. Carru, R. Madeddu, L. Murgia, F. Sgarrella, H. Dumortier and A. Bianco, *Nanomedicine*, 2012, **7**, 231–243.
16 M. Pescatori, D. Bedognetti, E. Venturelli, C. Ménard-Moyon, C. Bernardini, E. Muresu, A. Piana, G. Maida, R. Manetti, F. Sgarrella, A. Bianco and L. G. Delogu, *Biomaterials*, 2013, **34**, 4395–4403.
17 C. Crescio, M. Orecchioni, C. Ménard-Moyon, F. Sgarrella, P. Pippia, R. Manetti, A. Bianco and L. G. Delogu, *Nanoscale*, 2014, **6**, 9599–9603.
18 C. A. Poland, R. Duffin, I. Kinloch, A. Maynard, W. A. H. Wallace, A. Seaton, V. Stone, S. Brown, W. Macnee and K. Donaldson, *Nat. Nanotechnol.*, 2008, **3**, 423–428.
19 K. Kostarelos, *Nat. Biotechnol.*, 2008, **26**, 774–776.
20 K. Kostarelos, *Nat. Mater.*, 2010, **9**, 793–795.
21 J. E. Podesta, K. T. Al-Jamal, M. A. Herrero, B. Tian, H. Ali-Boucetta, V. Hegde, A. Bianco, M. Prato and K. Kostarelos, *Small*, 2009, **5**, 1176–1185.
22 K. T. Al-Jamal, L. Gherardini, G. Bardi, A. Nunes, C. Guo, C. Bussy, M. A. Herrero, A. Bianco, M. Prato, K. Kostarelos and T. Pizzorusso, *Proc. Natl. Acad. Sci. U. S. A.*, 2011, **108**, 10952–10957.
23 C. Guo, W. T. Al-Jamal, F. M. Toma, A. Bianco, M. Prato, K. T. Al-Jamal and K. Kostarelos, *Bioconjugate Chem.*, 2015, **26**, 1370–1379.
24 A. Akinc, A. Zumbuehl, M. Goldberg, E. S. Leshchiner, V. Busini, N. Hossain, S. A. Bacallado, D. N. Nguyen, J. Fuller, R. Alvarez, A. Borodovsky, T. Borland, R. Constien, A. de Fougerolles, J. R. Dorkin, K. Narayanannair Jayaprakash, M. Jayaraman, M. John, V. Koteliansky, M. Manoharan, L. Nechev, J. Qin, T. Racie, D. Raitcheva, K. G. Rajeev, D. W. Y. Sah, J. Soutschek, I. Toudjarska, H.-P. Vornlocher, T. S. Zimmermann, R. Langer and D. G. Anderson, *Nat. Biotechnol.*, 2008, **26**, 561–569.
25 P. Y. Lu and M. C. Woodle, *Methods Mol. Biol.*, 2008, **437**, 93–107.
26 T. Nguyen, E. M. Menocal, J. Harborth and J. H. Fruehauf, *Curr. Opin. Mol. Ther.*, 2008, **10**, 158–167.
27 A. Battigelli, J. T.-W. Wang, J. Russier, T. Da Ros, K. Kostarelos, K. T. Al-Jamal, M. Prato and A. Bianco, *Small*, 2013, **9**, 3610–3619.
28 G. Bardi, A. Nunes, L. Gherardini, K. Bates, K. T. Al-Jamal, C. Gaillard, M. Prato, A. Bianco, T. Pizzorusso and K. Kostarelos, *PLoS One*, 2013, **8**, e80964.
29 A. Hirsch, *Angew. Chem., Int. Ed.*, 2002, **41**, 1853.
30 S. Niyogi, M. A. Hamon, H. Hu, B. Zhao, P. Bhowmik, R. Sen, M. E. Itkis and R. C. Haddon, *Acc. Chem. Res.*, 2002, **35**, 1105–1113.
31 C.-H. Andersson and H. Grennberg, *Eur. J. Org. Chem.*, 2009, 4421–4428.
32 T. Ramanathan, F. T. Fisher, R. S. Ruoff and L. C. Brinson, *Chem. Mater.*, 2005, **17**, 1290–1295.
33 A. Gromov, S. Dittmer, J. Svensson, O. A. Nerushev, S. A. Perez-García, L. Licea-Jiménez, R. Rychwalski and E. E. B. Campbell, *J. Mater. Chem.*, 2005, **15**, 3334.
34 L. Wang, S. Feng, J. Zhao, J. Zheng, Z. Wang, L. Li and Z. Zhu, *Appl. Surf. Sci.*, 2010, **256**, 6060–6064.
35 K. S. Coleman, A. K. Chakraborty, S. R. Bailey, J. Sloan and M. Alexander, *Chem. Mater.*, 2007, **19**, 1076–1081.
36 K. T. Al-Jamal, F. M. Toma, A. Yilmazer, H. Ali-Boucetta, A. Nunes, M. A. Herrero, B. Tian, A. Eddaoui, A. Bianco, M. Prato and K. Kostarelos, *FASEB J.*, 2010, **24**, 4354–4365.
37 C. Samorì, R. Sainz, C. Ménard-Moyon, F. M. Toma, E. Venturelli, P. Singh, M. Ballestri, M. Prato and A. Bianco, *Carbon*, 2010, **48**, 2447–2454.
38 J. Zhang, H. Zou, Q. Qing, Y. Yang, Q. Li, Z. Liu, X. Guo and Z. Du, *J. Phys. Chem. B*, 2003, **107**, 3712–3718.

39 D. Bonifazi, C. Nacci, R. Marega, S. Campidelli, G. Ceballos, S. Modesti, M. Meneghetti and M. Prato, *Nano Lett.*, 2006, **6**, 1408–1414.
40 M. B. Smith and J. March, *March's Advanced Organic Chemistry: Reactions, Mechanisms and Structure*, John Wiley & Sons Inc., New Jersey, 6th edn, 2007, vol. 2007.
41 D. Naskar, S. Chowdhury and S. Roy, *Tetrahedron Lett.*, 1998, **39**, 699–702.
42 D. Naskar and S. Roy, *Tetrahedron*, 2000, **56**, 1369–1377.
43 J. P. Das and S. Roy, *J. Org. Chem.*, 2002, **67**, 7861–7864.
44 E. Kaiser, R. L. Colescott, C. D. Bossinger and P. I. Cook, *Anal. Biochem.*, 1970, **34**, 595–598.
45 V. Datsyuk, M. Kalyva, K. Papagelis, J. Parthenios, D. Tasis, A. Siokou, I. Kallitsis and C. Galiotis, *Carbon*, 2008, **46**, 833–840.
46 C. Moreno-Castilla, M. V. López-Ramón and F. Carrasco-Marín, *Carbon*, 2000, **38**, 1995–2001.
47 S. Biniak, G. Szymański, J. Siedlewski and A. Świątkowski, *Carbon*, 1997, **35**, 1799–1810.
48 G. Ovejero, J. L. Sotelo, M. D. Romero, A. Rodríguez, M. A. Ocaña, G. Rodríguez and J. García, *Ind. Eng. Chem. Res.*, 2006, **45**, 2206–2212.
49 S. Goyanes, G. R. Rubiolo, A. Salazar, A. Jimeno, M. A. Corcuera and I. Mondragon, *Diamond Relat. Mater.*, 2007, **16**, 412–417.
50 A. Fire, S. Xu, M. K. Montgomery, S. A. Kostas, S. E. Driver and C. C. Mello, *Nature*, 1998, **391**, 806–811.
51 S. M. Elbashir, J. Harborth, W. Lendeckel, A. Yalcin, K. Weber and T. Tuschl, *Nature*, 2001, **411**, 494–498.
52 A. de Fougerolles, H.-P. Vornlocher, J. Maraganore and J. Lieberman, *Nat. Rev. Drug Discovery*, 2007, **6**, 443–453.